Yonsei Med J 48(5):818 - 826, 2007
DOI 10.3349/ymj.2007.48.5.818

Diagnosis of the Double Aortic Arch and Its Differentiation from the Conotruncal Malformations

Meng-Luen Lee

Department of Pediatrics, Division of Pediatric Cardiology and Director of Pediatric Intensive Care Unit, Changhua Christian Hospital, Changhua 50050, Taiwan.

Purpose: The clinical and radiological characteristics of the double aortic arch (DAA) and its differentiation from conotruncal malformations (CTM) were reported in order to familiarize pediatric practitioners with these congenital heart diseases. **Materials and Methods:** From July 1994 to December 2006, a total of 6 patients (4 male and 2 female, aged 16 days to 6.5 years) with DAA were enrolled in this retrospective study. The study modalities included chart recordings, plain chest radiographs, barium esophagograms, echocardiograms, cardiac catheterization, cardiac angiograms, surgery, magnetic resonance imaging, and chromosome analysis. Patients with incomplete vascular rings or with right aortic arches and left ligamentum were excluded. In addition, the clinical and radiological profiles of 38 patients with CTM, including dextro-transposition of the great arteries (d-TGA) (n = 28), hemitruncus arteriosus (HTA) (n = 3), type I truncus arteriosus (TA) (n = 4), and the aortopulmonary window (APW) (n = 3), were comparatively reviewed. **Results:** All 6 patients with DAA presented with postprandial choking and respiratory distress that prompted their initial visit to the hospital. One of the 6 patients presented with congestive heart failure, and none with cyanosis. Esophagograms showed indentations in 5 patients with DAA. All patients with d-TGA presented with cyanosis and heart failure, while patients with HTA, type I TA, and APW manifested overt heart failure. Suprasternal and subcostal approaches of the echocardiography may offer diagnositic windows for DAA. As for CTM, parasternal and subcostal approaches could always determine the causality. Cardiac catheterization with angiography comprehensively delineated the pathology. **Conclusion:** In case of postprandial choking and respiratory distress in neonates and infants, barium esophagograms can indicate the presence of DAA. Diagnosis of DAA and its differentiation from the CTM can be achieved by echocardiography, angiography, or magnetic resonance imaging.

Key Words: Double aortic arch, conotruncal malformations, dextro-transposition of the great arteries, hemitruncus arteriosus, truncus arteriosus, aortopulmonary window, barium esophagogram, echocardiography, angiography, magnetic resonance imaging

INTRODUCTION

DAA is usually an isolated aortic arch anomaly and is rarely (7% to 17%) associated with other congenital heart diseases.[1,2] DAA may manifest as respiratory distress and feeding problems early in life. The cardinal features of respiratory distress and feeding problems, which are not uncommonly encountered in patients with isolated DAA, can be masked by the overwhelming cyanosis or congestive heart failure is frequently seen in patients with DAA associated with other major cardiovascular malformations. In this retrospective study, the clinical, radiographic, echocardiographic, angiographic, and magnetic resonance imaging (MRI) characteristics of isolated and complex DAA and its differentiation from the d-TGA, HTA, type I TA, and APW were reported to familiarize pediatric practitioners with these congenital heart diseases.

MATERIALS AND METHODS

From July 1, 1994 to December 31, 2006, a total of 6 patients (4 male and 2 female, aged 16 days to 6.5 years) with DAA and 38 patients with CTM, including d-TGA (n = 28), HTA (n = 3), type I TA

Received January 19, 2007
Accepted March 23, 2007

Reprint address: requests to Dr. Meng-Luen Lee, Department of Pediatrics, Division of Pediatric Cardiology, Changhua Christian Hospital, No. 135, Nanhsiao St., Changhua 50050, Taiwan. Tel: 886-4-7238595 (1902), Fax: 886-4-7238847, E-mail: ferdielee@yahoo.com

(n = 4), and APW (n = 3) were included in this retrospective survey. Patients with incomplete vascular rings, or right aortic arch with left ligamentum were excluded.[3] To support the diagnosis of DAA, d-TGA, HTA, type I TA, or APW, we monitored the patients with chart recordings (n = 44), plain chest films (n = 44), plus at least 2 of the following study modalities: two-dimensional echocardiography with Doppler (Acuson 128XP/10c, Mountain View, CA, USA) (n = 44), cardiac catheterization with angiography (n = 44), surgery (n = 42), MRI (n = 2), barium esophagography (n = 6), and chromosome analysis (n = 2).

Echocardiograms and angiocardiograms of patients with the DAA were compared with those of the patients with d-TGA, HTA, type I TA, and APW. The absolute bifurcation distance, from semilunar aortic valve to pulmonary bifurcation (d-TGA, HTA, and APW), or from truncal valve to aortopulmonary bifurcation (type I TA) was measured directly by the echocardiographic calipers or indirectly by the angiographic calipers after calibration of the catheter. This absolute distance was corrected for body surface area (BSA) in terms of mm/m^2. Magnetic resonance imaging studies were performed on 2 patients with DAA to delineate the associated intracardiac lesions. To confirm diagnosis of the 22q11 deletion syndrome, cytogenetic analysis and fluorescence in situ hybridization (FISH) studies were performed on 2 patients presenting with the clinical stigmata of DiGeorge sequences. One patient had DAA and tetralogy of Fallot, and the other patient had APW, type B aortic interruption, patent ductus arteriosus, and ventricular septal defects.

RESULTS

All 4 male and 2 female patients, aged between 16 days and 6.5 years, had a remarkable history of respiratory distress and postprandial choking since birth. Two patients had isolated DAA, while four had associated complex cardiovascular malformations. Recurrent infections of the lower respiratory tract were noted in 5 patients with DAA. A 16-day-old neonate with 22q11 deletion syndrome did not manifest recurrent lung infection due to the early diagnosis and repair of the DAA and the tetralogy of Fallot. Remarkable cyanosis was found in 3 patients since birth, which were caused by intracardiac anomalies rather than DAA. One of these patients had tetralogy of Fallot and the 22q11 deletion syndrome, one had tetralogy of Fallot and absent pulmonary valve syndrome, and one had tricuspid atresia and pulmonary atresia. Congestive heart failure was noted in one patient with large ventricular septal defects. Inspiratory stridor was noted in 4 patients and expiratory wheezing lingered in the patient with the tetralogy of Fallot and the absent pulmonary valve syndrome, a syndrome which is usually associated with respiratory problems. Dysphagia was found in 3 children. Two out of the 6 patients tolerated respiratory and feeding problems from birth to 14 and 15.5 years of age, respectively. Plain chest films showed a suspicious contour of the right aortic arch in 2 patients (Fig. 1A) and deviation of the trachea in 1 patient (Fig. 1B). Barium esophagograms, which were performed in 5 patients, showed an indentation of the esophagus (Figs. 1C and D). DAA was appreciated before

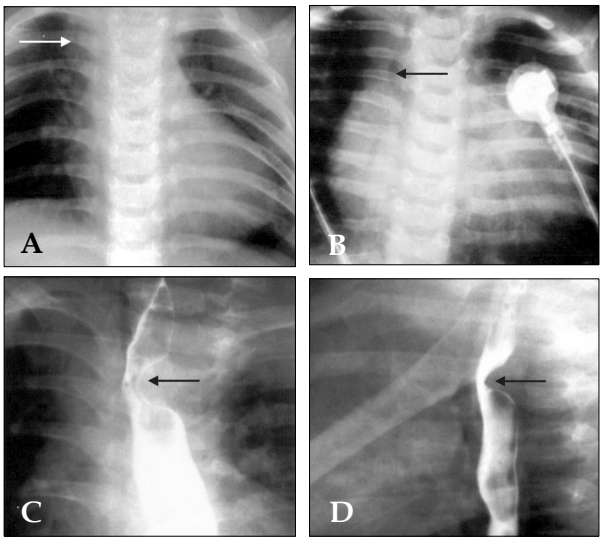

Fig. 1. Plain chest radiographs showed a bulged contour (arrow) at the right upper cardiac border of a 4.5-month-old male (A), and deviations (arrow) of the trachea in a 16-day-old male (B). Barium esophagograms taken from a 4.5-month-old male showed an indentation (arrow) at the upper third portion of the esophagus, which is located on the left aspect of the frontal projection (C), and the posterior aspect of the lateral projection (D), respectively.

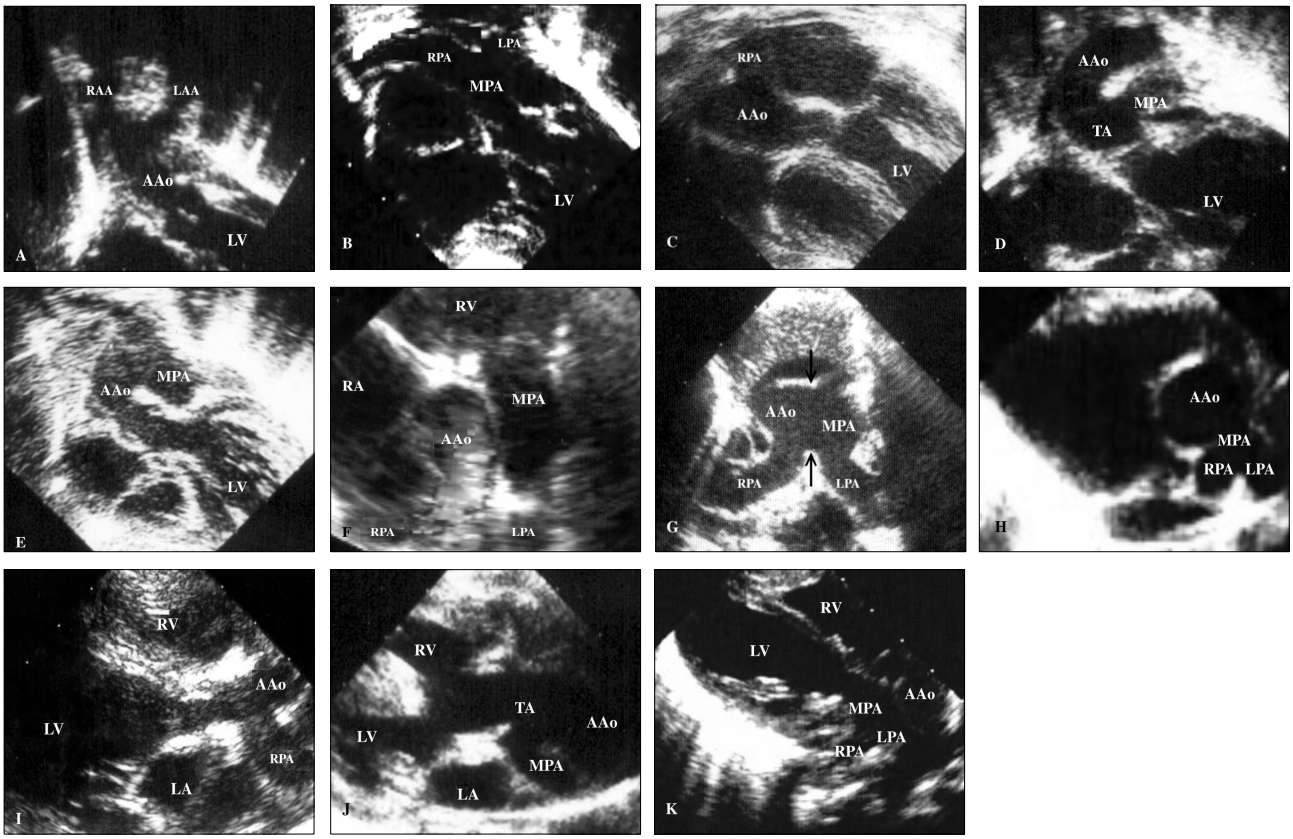

Fig. 2. Subcostal view of the left ventricular outflow tract of echocardiography showed a characteristic morphology of the aortic bifurcations in cases with DAA (A), which has a longer bifurcation distance (from the semilunar valve to the site of bifurcation) than the bifurcation distance measured in cases with d-TGA (B), HTA (C), type I TA (D), and APW (E). Parasternal short-axis view showed an anomalous origin of the right pulmonary artery from the ascending aorta in a case of isolated HTA (F), and when complexed with APW (arrows) in the Berry syndrome (G), as well as an abnormal take-off of the main pulmonary artery from the left-posterior aspect of the aorta in cases with type I TA (H). Over the parasternal long-axis views, we may visualize bifurcation either from the ascending aorta, as in the case of HTA (I), or from the truncus in TA cases (J), which can be similar to d-TGA cases (K). AAo, ascending aorta; APW, aortopulmonary window; DAA, double aortic arch; d-TGA, dextro-transposition of the great arteries; HTA: hemitruncus arteriosus; LA, left atrium; LAA, left aortic arch; LPA, left pulmonary artery; LV, left ventricle; MPA, main pulmonary artery; RA, right atrium; RAA, right aortic arch; RPA, right pulmonary artery; TA, truncus arteriosus.

cardiac catheterization by two-dimensional echocardiography, in which suprasternal and subcostal views of the left ventricular outflow tract offered diagnostic windows for the DAA (Fig. 2A). As for CTM, subcostal and parasternal views can always determine the cause to be either d-TGA (Figs. 2B and K), HTA (Figs. 2C, F and I), type I TA (Figs. 2D, H, and J), or APW (Figs. 2E and G). The ascending aortography showed a bifurcated, or Y-shaped double aortic arch (Figs. 3A and B), with a dominant right arch, and a smaller left arch in 5 patients. One patient had balanced aortic arches. Left ventriculography of the d-TGA patients (Fig. 3C), and ascending aortography of the HTA, (Fig. 3D), type I TA (Figs. 3E and F), and APW (Fig. 3G) patients demonstrated that the bifurcations originated from one great artery, either the main pulmonary artery or the ascending aorta, which was committed to the left ventricle. Magnetic resonance imaging studies, which were performed in 2 patients with complex DAA, showed a bifurcated or Y-shaped double aortic arch, with a dominant right arch and a smaller left arch (Fig. 4). All but 2 patients underwent surgery at the time of presentation and diagnosis. Four (2 with isolated DAA, 1 complicated with VSD, and 1 with tetralogy of Fallot and 22q11 deletion syndrome) out of the six patients with DAA

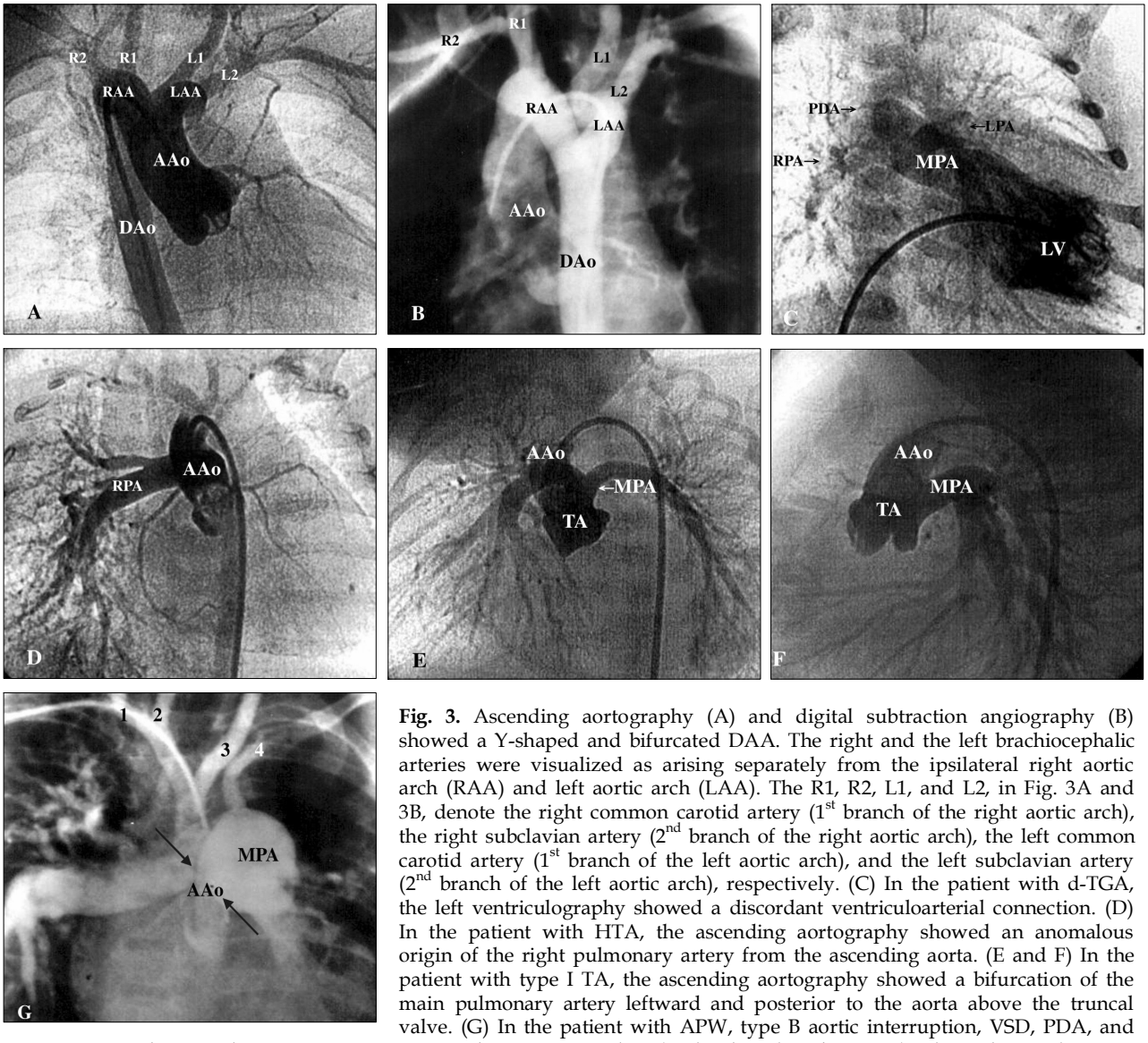

Fig. 3. Ascending aortography (A) and digital subtraction angiography (B) showed a Y-shaped and bifurcated DAA. The right and the left brachiocephalic arteries were visualized as arising separately from the ipsilateral right aortic arch (RAA) and left aortic arch (LAA). The R1, R2, L1, and L2, in Fig. 3A and 3B, denote the right common carotid artery (1st branch of the right aortic arch), the right subclavian artery (2nd branch of the right aortic arch), the left common carotid artery (1st branch of the left aortic arch), and the left subclavian artery (2nd branch of the left aortic arch), respectively. (C) In the patient with d-TGA, the left ventriculography showed a discordant ventriculoarterial connection. (D) In the patient with HTA, the ascending aortography showed an anomalous origin of the right pulmonary artery from the ascending aorta. (E and F) In the patient with type I TA, the ascending aortography showed a bifurcation of the main pulmonary artery leftward and posterior to the aorta above the truncal valve. (G) In the patient with APW, type B aortic interruption, VSD, PDA, and DiGeorge syndrome, the countercurrent ascending aortography (with digital subtraction) showed simultaneous opacification of the pulmonary arteries through the aortopulmonary defect (arrows) and interruption of the aortic arch between the left common carotid artery and the left subclavian artery. The Arabic numerals 1, 2, 3, and 4, in Fig. 3G, denote the right subclavian artery, right common carotid artery, left common carotid artery, and left subclavian artery, respectively. AAo, ascending aorta; APW, aortopulmonary window; DAA, double aortic arch; DAo, descending aorta; d-TGA, dextro-transposition of the great arteries; HTA: hemitruncus arteriosus; LAA, left aortic arch; LV, left ventricle; MPA, main pulmonary artery; PDA, patent ductus arteriosus; RAA, right aortic arch; RPA, right pulmonary artery; TA, truncus arteriosus; VSD, ventricular septal defect.

survived the surgical division of the smaller left aortic arch. The former 3 surviving patients were repaired by a one-stage surgery, and the latter surviving patient was repaired by a two-stage procedure. Surgical interventions were declined by the parents of the remaining two patients, one with the absent pulmonary valve syndrome and one with tricuspid atresia as well as pulmonary atresia. The two patients, who did not undergo surgery, could tolerate mild cyanosis, exertional dyspnea, and dysphagia in their daily activities. At the time of this report, these two patients continue to survive without surgical correction and have oxygen saturations between 80% and 85%.

All patients with d-TGA (n=28) presented with

remarkable cyanosis, while patients with HTA (n = 3), type I TA (n = 4), and APW (n = 3) manifested overt congestive heart failure. Among the 3 patients with HTA, 2 had isolated lesions and one had associated Berry syndrome. All 4 patients with type I TA had associated large ventricular septal defects. In 3 patients with APW, one patient had isolated APW, one patient had APW associated with the 22q11 deletion syndrome (DiGeorge sequences, type B aortic interruption, patent ductus arteriosus, and ventricular septal defect), and one patient had APW associated with the Berry syndrome (type A aortic interruption, patent ductus arteriosus, ventricular septal defect, and hemitruncus arteriosus). Patients with DAA had a much longer bifurcation distance and a larger bifurcation distance/BSA ratio (bifurcation distance 20-66 mm, median 45 mm; bifurcation distance/BSA ratio 72-114 mm/m^2, median 97 mm/m^2; patient age, 16 days to 6.5 years old) than those measured in the patients with CTM (bifurcation distance 5-10 mm, median 8 mm; bifurcation distance/BSA ratio 24-55 mm/m^2, median 42 mm/m^2; within 7 days of life), including the patients with d-TGA (10 mm/0.181 m^2 = 55 mm/m^2), HTA (9 mm/0.195 m^2 = 46 mm/m^2), type I TA (5 mm/0.208 m^2 = 24 mm/m^2), and APW (8 mm/0.189 m^2 = 42 mm/m^2).

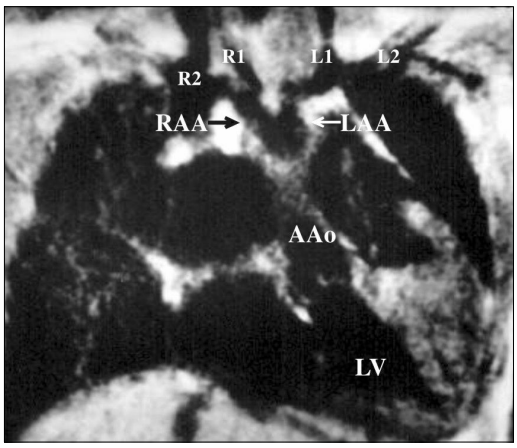

Fig. 4. Magnetic resonance imaging in a 6.5-year-old boy visualized that the right and the left brachiocephalic arteries arose separately from the ipsilateral right aortic arch (RAA) and left aortic arch (LAA). The R1, R2, L1, and L2 denote the right common carotid artery (1st branch of the right aortic arch), right subclavian artery (2nd branch of the right aortic arch), left common carotid artery (1st branch of the left aortic arch), and left subclavian artery (2nd branch of the left aortic arch), respectively.

Table 1. Diagnosis of the Double Aortic Arch and Its Differentiation from the Conotruncal Malformations

DAA (a, b)	Clinical features	Echocardiographic views		
		Suprasternal long-axis	Suprasternal short-axis	Subcostal LVOT
a. Isolated b. Complex	a. Respiration b. It depends	[1] A LAA with LCCA (1st branch) and LSCA (2nd branch) in LOP [2] A RAA with RCCA (1st branch) and RSCA (2nd branch) in ROP	A ring of double arches	Centripetal bifurcation of the Ao (> 4 cm above the aortic valve) to form two embracing aortic arches
CTM (1-4)		Parasternal long-axis	Parasternal short-axis	Subcostal LVOT
1. D-TGA	CHF and Cyanosis	MPA committed to LV	Ao is right-anterior to MPA	MPA is committed to LV
2. HTA	CHF	RPA from the Ao	RPA from the Ao LPA from the MPA	A bifurcated branch from the Ao as RPA
3. TA	CHF > Cyanosis	A TA bifurcates as 2 great arteries, committed to LV	MPA is arising from the left-posterior aspect of Ao	A TA bifurcates as 2 great arteries, committed to LV
4. APW	CHF > Cyanosis	Not yielding in this view	A defect at distal APS	A defect at distal APS

Ao, aorta; APS, aortopulmonary septum; APW, aortopulmonary window; CHF, congestive heart failure; DAA, double aortic arch; d-TGA, dextro-transposition of the great arteries; HTA: hemitruncus arteriosus; LAA, left aortic arch; LCCA, left common carotid artery; LOP, left oblique plane; LSCA, left subclavian artery; LV, left ventricle; LVOT, left ventricular outflow tract; MPA, main pulmonary artery; RAA, right aortic arch; RCCA, right common carotid artery; ROP, right oblique plane; RPA, right pulmonary artery; RSCA, right subclavian artery; TA, truncus arteriosus.

The clinical and echocardiographic characteristics of DAA and the characteristics that differentiate DAA from CTM are summarized in Table 1.

DISCUSSION

DAA is the most frequently encountered vascular ring malformation that inevitably completely encircles the trachea and esophagus.[1] The DAA, together with the right aortic arch with left ligamentum, is defined anatomically as the complete vascular ring.[3] DAA is usually found as an isolated cardiovascular malformation. Associated cardiac anomalies occurred only in 8 patients (7%) in a large study of 113 patients with DAA[1] and appeared in 14 patients (17%) in another study of 81 patients with DAA.[2] Among these associated cardiac anomalies, ventricular septal defects rank first, atrial septal defects follow at distant second, while patent ductus arteriosus, tetralogy of Fallot, d-TGA, and many others follow far behind.[2-14]

The cardinal manifestations of respiratory distress and feeding problems, which are commonly encountered in patients with isolated DAA, can be masked by the overwhelming features of cyanosis or congestive heart failure that is often seen in patients with DAA complicated by other intracardiac anomalies. For example, in patients that have DAA intricated with tetralogy of Fallot,[4,5] d-TGA,[6-8] tricuspid atresia, and pulmonary atresia, they will also have overt cyanosis rather than respiratory distress, postprandial choking, and aspiration pneumonia. Patients with large ventricular septal defects, truncus arteriosus,[9] patent ductus arteriosus,[10] coarctation of the aortic arch,[11-13] and supravalvular mitral stenosis with subvalvular aortic stenosis, and ventricular septal defects[14] may present with discernible congestive heart failure rather than with the above major features of respiratory and gastroesophageal symptoms. The clinical or diagnostic spectrum of a vascular ring may range from severely compromised respiratory and gastroesophageal symptoms in newborns with complete vascular rings (DAA or right aortic arch with left ligamentum) to freedom from symptoms in adults with incomplete rings due to an aberrant subclavian artery. In every newborn or child with stridor, wheezing, and dysphagia, the presence of a complete vascular ring should be carefully identified. In asymptomatic adults, the diagnosis of an incomplete vascular ring is usually made by chance.

Many radiological modalities can provide important clues toward a diagnosis of DAA. First of all, plain chest radiographs may show a deviation or compression of the trachea, or contour of a right arch, especially in the scenario of an infant presenting with respiratory and gastroesophageal symptoms. Barium esophagography has been advocated as a valuable investigation for patients with suspected vascular rings, because it can be safely and rapidly performed to diagnose DAA with high sensitivity. Barium esophagograms were once considered the single most important or the primary method of study in evaluating patients with vascular rings.[15,16] However, this method is no longer considered a sufficient evaluation of the patient before proceeding with treatment by vascular ring repair.[1] This trend in imaging diagnosis for vascular rings may change because of the increasing ease and safety provided by computed tomography (CT) and MRI and the ability of these methods to improve patient outcome through their precise ability to plan operative procedures.[1] Compared to CTs and MRIs, barium esophagograms cannot provide a clear surgical "road map" that can generate a precise preoperative strategy,[1] especially in patients with typical vascular ring formations that necessitate using a right thoracotomy for surgical treatment.[17-19] For the evaluation of patients with vascular rings, CT and MRI could be used as valid alternative methods to barium esophagograms and angiographies.[20,21] This dramatic shift from barium esophagograms and angiographies to CTs and MRIs in the preoperative evaluation strategy of 209 patients with complete vascular rings (113 patients with DAA and 96 with right aortic arch and left ligamentum) may be stemmed from the following: 1) referrals were generated by otolaryngology instead of pediatric cardiology, 2) a significant number of patients with right aortic arches with left ligamentum, 3) the unusual anatomy of a right

aortic arch with a left ligamentum, retroesophageal left subclavian artery, and large Kommerell diverticulum, and 4) the inability of the echocardiographers to identify useful anatomic details.[1] However, these updated options shall not lead us to leave the echocardiography and barium esophagograms in the niche.

Two-dimensional echocardiography can usually substantiate a diagnosis of DAA. Furthermore, echocardiography is very useful for identifying associated congenital heart diseases. Subcostal[22] and suprasternal[23,24] views of the two-dimensional echocardiography may offer diagnostic windows for pediatric practitioners or cardiologists to assess patients with DAA. The subcostal view of the left ventricular outflow tract can be used to visualize aortic bifurcation, which was 40 mm and 45 mm above the aortic valve in 2 infants. This bifurcation generates a Y-shaped, centripetal, and embracing morphology.[22] We cannot overemphasize that the subcostal approach is practical only in infants younger than 12 months old, especially in neonates. A major drawback of the subcostal approach is that the area of interest is confined to far-field imaging, which can be given a reduced resolution in larger patients. The suprasternal notch approach can overcome this problem by imaging the area of interest in the near field. By a suprasternal notch long-axis/sagittal plane (with leftward obliquity) and a 30 degrees counterclockwise rotation of the transducer (with rightward obliquity), we can visualize a left arch and a right arch, respectively. In each oblique plane, we can see only 2 head and neck arteries, i.e., carotid (1st branch) and subclavian (2nd branch) arteries, arising sequentially and ipsilaterally from each corresponding arch.[25] Then, a suprasternal notch short-axis/coronal plane can be used to track down the possible culprit to be a DAA by using one scanning plane. We shall not jump to display both arches in one suprasternal notch short-axis/coronal plane without identifying the branching pattern of each arch in the suprasternal notch long-axis or sagittal plane *a priori*. Jumping to the conclusion of a DAA diagnosis by only performing a suprasternal notch short-axis/coronal view is risky, due to the large number of false positive images which are caused by a "phantom" right pulmonary artery aliasing as a vascular ring. In the hands of experienced investigators, transthoracic echocardiography permits an accurate imaging of DAA and any associated congenital heart diseases as well as clear identification of the sidedness of the aortic arch. The major problem resides in its limited ability to image clearly the atretic aortic arch structures and a ligamentum arteriosum. Nonetheless, echocardiography remains a powerful, useful, and non-invasive tool that is capable of evaluating patients with suspected DAA.

From the subcostal view of the left ventricular outflow tract, we can differentiate the DAA from the d-TGA, HTA, type I TA, and APW by visualizing a centripetal morphology of the aortic bifurcation and by measuring the bifurcation distance. The aorta bifurcates at a strikingly longer distance beyond the aortic valve in patients with DAA. Such characteristic morphology can be easily differentiated from the pulmonary arterial bifurcation morphology seen in d-TGA cases[22] and the anomalous take-off morphology of the aortic pulmonary artery, namely, hemitruncus arteriosus, truncus arteriosus, and APW. With the *provisos* of patients' symptoms and esophageal indentations, the subcostal and suprasternal echocardiographic views offer diagnostic windows for DAA.[9,22,23] By the subcostal approach, we have found that these two bifurcations "embrace" each other centripetally in patients with DAA. From the embryogenetic viewpoints, the bifurcation distance from the semilunar valves to the pulmonary or aorticopulmonary bifurcations should be shorter than the bifurcation distance observed in DAA cases.[22,26] All these differences can be derived from embryogenesis due to branchial arch defects in DAA cases and conotruncal septation defects in patients with other malformations.[26] By approaching from the suprasternal notch, echocardiography can identify the dominant arch, the nature of each arch, and its branches.[22-25] Parasternal long and/or short- axis views and subcostal left ventricular outflow tract views are helpful in excluding DAA from a diagnosis, since early bifurcation is seen in one of the great arteries in patients with d-TGA, HTA, type I HA, and APW.

Although cardiac catheterization with angiography can provide a diagnosis of DAA and a

differential diagnosis of rare types of aortic arch anomalies, pulmonary slings, and ductal slings,[27-31] catheterization is neither routinely required nor clinically feasible for smaller patients with severe cardiopulmonary distress. Instead, CTs and MRIs can be performed non-invasively and safely, especially in patients compromised with severe cardiac or pulmonary failure. CTs and MRIs, which can image the atretic aortic segments, are of great value for preoperative planning.[1]

In patients with isolated DAA, surgical division of the smaller aortic arch is indicated. However, preoperative recognition of associated anomalies is important, especially in cases with coarctation or atresia of one or both arches, associated major congenital heart diseases, tracheomalacia, and bronchomalacia. On the one hand, surgical division of one aortic arch, without preoperative recognition of coarctation or atresia of the other arch, will make clinical care demanding and can be life threatening. On the other hand, in patients associated with other congenital heart diseases, e.g., tetralogy of Fallot, d-TGA, HTA, HA, and APW, which may dominate the clinical manifestations with cyanosis and heart failure, the symptoms of DAA may be too subtle to appreciate. Finally, a preoperative bronchoscopy can be used to rule out associated tracheomalacia or bronchomalacia and is important to the patient's short- and long-term prognosis.[1] Thus, echocardiography, angiography, bronchoscopy, CT, and MRI can be selectively employed to evaluate the detailed anatomy of the aortic arches and airways in patients with DAA.

In conclusion, visualization of the contour of a right aortic arch with or without tracheal deviation on plain chest radiographs of infants presenting with respiratory and gastroesophageal symptoms may lead to an early suspicion of DAA. Altogether, barium esophagography, echocardiography, angiography, bronchoscopy, CT, and MRI can be applied individually to evaluate the detailed pathology of the aortic arches, airways, and the associated congenital heart diseases as well as permit a detailed planning of successful surgical correction in patients with DAA.

REFERENCES

1. Backer CL, Mavroudis C, Rigsby CK, Holinger LD. Trends in vascular ring surgery. J Thorac Cardiovasc Surg 2005;129:1339-47.
2. Alsenaidi K, Gurofsky R, Karamlou T, Williams WG, McCrindle BW. Management and outcomes of double aortic arch in 81 patients. Pediatrics 2006;118:e1336-41.
3. Backer CL, Mavroudis C. Congenital Heart Surgery Nomenclature and Database Project: vascular rings, tracheal stenosis, pectus excavatum. Ann Thorac Surg 2000;69(4 Suppl):S308-18.
4. Blumenthal S, Ravitch MM. Seminar on aortic vascular rings and other anomalies of the aortic arch. Pediatrics 1957;20:896-906.
5. Griswold HE, Young MD. Double aortic arch; Report of two cases and review of the literature. Pediatrics 1949;4:751-68.
6. Burrows PE, Moes CA, Freedom RM. Double aortic arch with atretic right dorsal segment. Pediatr Cardiol 1986;6:331-4.
7. Hawker RE, Celermajer JM, Cartmill TB, Bowdler JD. Double aortic arch and complex cardiac malformations. Br Heart J 1972;34:1311-3.
8. Higashino SM, Ruttenberg HD. Double aortic arch associated with complete transposition of the great vessels. Br Heart J 1968;30:579-81.
9. Alboliras ET, Lombardo S, Antillon J. Truncus arteriosus with double aortic arch: two-dimensional and color flow Doppler echocardiographic diagnosis. Am Heart J 1995;129:415-7.
10. Shirali GS, Geva T, Ott DA, Bricker JT. Double aortic arch and bilateral patent ducti arteriosi associated with transposition of the great arteries: missing clinical link in an embryologic theory. Am Heart J 1994;127:451-3.
11. Okuda Y, Takeda k, Ooi M, Nakagawa T, Yamaguchi N. Double aortic arch associated with coarctation of both limbs: a case report. Angiology 1991;42:760-4.
12. Singer SJ, Fellows KE, Jonas RA. Double aortic arch with bilateral coarctations. Am J Cardiol 1988;61:196-7.
13. Ettedgui JA, Lorber A, Anderson D. Double aortic arch associated with coarctation. Int J Cardiol 1986;12:258-60.
14. Gilbert G, Aerichide N, Bourassa M, David P. Supravalvular mitral stenosis associated with ventricular septal defect, subvalvular aortic stenosis and double aortic arch. Am J Cardiol 1966;18:605-9.
15. Backer CL, Ilbawi MN, Idriss FS, DeLeon SY. Vascular anomalies causing tracheoesophageal compression. Review of experiences in children. J Thorac Cardiovasc Surg 1989;97:725-31.
16. Stark J, Roesler M, Chrispin A, deLeval M. The diagnosis of airway obstruction in children. J Pediatr Surg 1985;20:113-7.
17. McFaul R, Millard P, Nowicki E. Vascular rings necessitating right thoracotomy. J Thorac Cardiovasc Surg 1981;82:306-9.
18. Whitman G, Stephenson LW, Weinberg P. Vascular

ring: left cervical aortic arch, right descending aorta, and right ligamentum arteriosum. J Thorac Cardiovasc Surg 1982;83:311-5.
19. Robotin MC, Bruniaux J, Serraf A, Uva MS, Roussin R, Lacour-Gayet F, et al. Unusual forms of tracheobronchial compression in infants with congenital heart disease. J Thorac Cardiovasc Surg 1996;112:415-23.
20. Lee EY, Siegel MJ, Hildebolt CF, Gutierrez FR, Bhalla S, Fallah JH. MDCT evaluation of thoracic aortic anomalies in pediatric patients and young adults: comparison of axial, multiplanar, and 3D images. AJR Am J Roentgenol 2004;182:777-84.
21. Weinberg PM. Aortic arch anomalies. J Cardiovasc Magn Reson 2006;8:633-43.
22. Sahn DJ, Valdes-Cruz LM, Ovitt TW, Pond G, Mammana R, Goldberg SF, et al. Two dimensional echocardiography and intravenous digital video subtraction angiography for diagnosis and evaluation of double aortic arch. Am J Cardiol 1982;50:342-6.
23. Enderlein MA, Silverman NH, Stanger P, Heymann MA. Usefulness of suprasternal notch echocardiography for diagnosis of double aortic arch. Am J Cardiol 1986;57:359-61.
24. Goldberg BB. Suprasternal ultrasonography. JAMA 1971;215:245-50.
25. Silverman NH. Pediatric Echocardiography. 1st ed. Chapter 16: Abnormalities of the aortic arch. Baltimore: Williams & Wilkins; 1993. p.405-25.
26. Clark EB. Growth, morphogenesis and function: the dynamics of cardiac development. In: Moller JH, Neal W, editors. Fetal, neonatal and infant heart disease. New York: Appleton-Century-Crofts; 1990. p.3-23.
27. Moes CA, Freedom RM. Rare types of aortic arch anomalies. Pediatr Cardiol 1993;14:93-101.
28. Tonkin IL, Elliott LP, Bargeron LM Jr. Concomitant axial cineangiography and barium esophagography in the evaluation of vascular rings. Radiology 1980;135:69-76.
29. Elliott LP, Bargeron LM Jr, Bream PR, Soto B, Curry GC. Axial cineangiography in congenital heart disease. Section II. Specific lesions. Circulation 1977;56:1048-93.
30. Moodie DS, Yiannikas J, Gill CC, Buonocore E, Pavlicek W. Intravenous digital subtraction angiography in the evaluation of congenital abnormalities of the aorta and aortic arch. Am Heart J 1982;104:628-34.
31. Tonkin IL, Gold RE, Moser D, Laster RE Jr. Evaluation of vascular rings with digital subtraction angiography. AJR Am J Roentgenol 1984;142:1287-91.